

Unveiling the Enigma: A Pictorial Review of Imaging Features in Hepatic and Extra- Hepatic Hydatid Disease

Pictorial Essay

Mahajan N*, Sankhe-Sonve A and Patil S

Department of Radiology, LTMMC and LTMGH, Sion, Mumbai, India

*Corresponding author: Nikhil Mahajan, Resident, Department of Radiology, LTMMC and LTMGH, Sion, Mumbai, India.

E-mail Id: nikhil697@gmail.com

Copyright: © 2024 Mahajan N, et al. This is an open access article distributed under the Creative Commons Attribution License, which permits unrestricted use, distribution, and reproduction in any medium, provided the original work is properly cited.

Article Information: Submission: 25/04/2024; Accepted: 08/07/2024; Published: 12/07/2024

Abstract

Hydatid disease is a zoonotic infection that is endemic in many parts of the world, mainly caused by the parasite *Echinococcus granulosus*, which primarily affects the liver and shows characteristic imaging features. However, hydatid disease is known to affect other organs, including spleen, kidney, lungs, heart, peritoneum, muscles, and brain. Laboratory serological findings and radiological features usually help establish the diagnosis of hydatid disease, however, hydatid cysts in unusual locations with atypical imaging features may complicate the differential diagnosis. Chest radiography (CXR), ultrasonography (USG), computed tomography (CT), and Magnetic resonance (MR) imaging help in the detection of the hydatid cysts in the liver and elsewhere as the imaging features of hydatid disease in extrahepatic locations frequently imitate features of hepatic hydatid disease. We propose various cases of hydatid disease with multiple locations.

Keywords: Hydatid; MRI; CT; Daughter Cysts; Gharbi

Introduction

Hydatid disease or echinococcosis, is a zoonotic infection caused by the larval stage of the tapeworm from genus *Echinococcus*. Among the various species included under this genus, those of medical importance are *E. granulosus* and *E. multilocularis*, associated with cystic echinococcosis and alveolar echinococcosis among humans. Radiological imaging plays a critical role in the diagnosis and management of hydatid disease, providing valuable information for the accurate characterization and localization of cystic lesions.

Hydatid cysts can affect the liver, lungs, brain, heart, kidneys, spleen, bones, and soft tissues, each presenting with unique radiological features. Ultrasonography is the primary imaging

modality for initial evaluation, offering a cost-effective and widely available method for assessing hydatid cysts' morphology and content [1]. Computed tomography (CT) is essential for providing precise anatomical location and detecting specific features such as daughter cysts, calcifications, and cyst wall thickness [2]. Magnetic resonance imaging (MRI) helps better soft tissue characterization, aiding in assessing complex hydatid cysts in various anatomical locations. This pictorial essay and literature review will highlight the key imaging features for the diagnosis of hydatid disease.

The hydatid cyst consists of three layers

- Pericyst: an outer fibrous capsule

- Ectocyst: an intermediate layer, made of acellular chitinous, laminated hyaline material
- Endocyst: The vital inner germinal layer giving rise to brood capsules and protoscolices.

Classification

The Pan American Health Organization (PAHO) and the WHO support the Gharbi’s and the WHO’s classification for diagnostic imaging, as explained briefly in (Table 1) [3].

Liver

Liver hydatid cysts can be solitary or multiple. On ultrasonography, hydatid cysts exhibit a “snowstorm sign” characterized by numerous echogenic foci that fall into the dependent portion of the cyst (Figure 5), which helps distinguish it from a true hepatic cyst[2]. On diffusion-weighted MR imaging, hydatid cysts have higher signal intensity than the liver parenchyma on high-b-value images and a

higher cyst-to-liver intensity ratio [4]. On USG, the cyst wall usually manifests as double echogenic lines separated by a hypoechogenic layer [1] (Figure 2).

The common complication observed with hepatic hydatid cysts is rupture and secondary infection. There are three types of cyst rupture, contained, communicating, and direct. In contained ruptures, the endocyst breaks, with collapse and wrinkling of the germinative membrane within the cyst, but the pericyst remains intact [5]. The typical imaging signs suggestive of contained rupture include the “waterlily sign”, “snake/serpent sign”, or the “snowstorm pattern” due to detached undulating membranes within the cyst that appear on ultrasound, CT, and MRI as serpentine floating linear membranes within the cyst [6]. A combination of hydatid sand and detached membranes manifested as a mixed echogenicity solid-appearing lesion on USG can represent a “Ball of Wool sign” (Figure 5) that can be distinguished from a solid tumor by Doppler ultrasound [7].

Communicating rupture indicates the passage of the cyst contents into the biliary radicles that have been incorporated into the pericyst [1]. The definitive sign of rupture into the biliary tree is the visualization of the cyst wall defect or communication between the cyst and a biliary radicle[8]. Hydatid cyst content into the biliary tract is noted as high attenuation/intensity content in the common bile duct on CT and T1-weighted MR imaging and as a hypointense filling defect on T2-weighted MR imaging or magnetic resonance cholangiopancreatography [6]. On MR imaging, using a hepatobiliary-specific contrast agent, a direct fistulous track could be noted between the hepatic hydatid cyst and biliary tree with leakage of the hepatobiliary contrast agent from the biliary tree into the hepatic hydatid cyst [9, 10]. The presence of intra-cystic fat due to the lipid content of the bile or air content and air-fluid levels are indirect signs of communicating rupture on CT and MRI [6]. Rupture of both pericyst and endocyst results in direct rupture with free spillage of hydatid material into the peritoneal cavity, pleural cavity, and so on [8].

Contrast-enhanced CT is the modality of choice for cyst infection which demonstrates poorly defined masses with typical high-attenuation rim representing abscesses surrounding the lesion [1, 11].

Hydatid cysts may progress beyond the boundaries of the liver via natural routes, most commonly the bare area of the liver and the

Table 1:

WHO classification	Gharbi classification	Stage	USG features
Type CL	----	Active	Nonspecific characteristics. Unilocular with homogeneous anechoic fluid content and non-visible wall. This type represents a hydatid cyst of early diagnosis and cannot be differentiated from the simple cyst. It is a fertile cyst.
Type CE1	Type I		Anechoic cyst with wall, hydatid sand with or without snowflake sign.
Type CE2	Type III	Transition	Multilocular septate cyst, honeycomb sign or spoke wheel sign
Type CE3A	Type II		Cyst with detached membrane
Type CE3B		Cyst with daughter vesicles in a solid matrix	
Type CE4	Type IV	Inactive	Cyst with heterogenous content with mainly solid components (no daughter cysts)
Type CE5	Type V		Partially or completely calcified cyst

CL: Cystic lesion
CE: Cystic Echinococcosis



Figure 1: Case of a 60-year-old female with right hypochondriac pain: Axial sections of non-contrast (Image A), contrast (Image B), and delayed phase (Image C) of CT abdomen respectively reveal a well-defined solid lesion in the right lobe of liver showing areas of calcification (hyperdense areas within cyst) and hypodense membranes (marked by white block arrow), with no enhancement and washout on contrast and delayed phase (WHO stage CE-4 or Gharbi type IV).

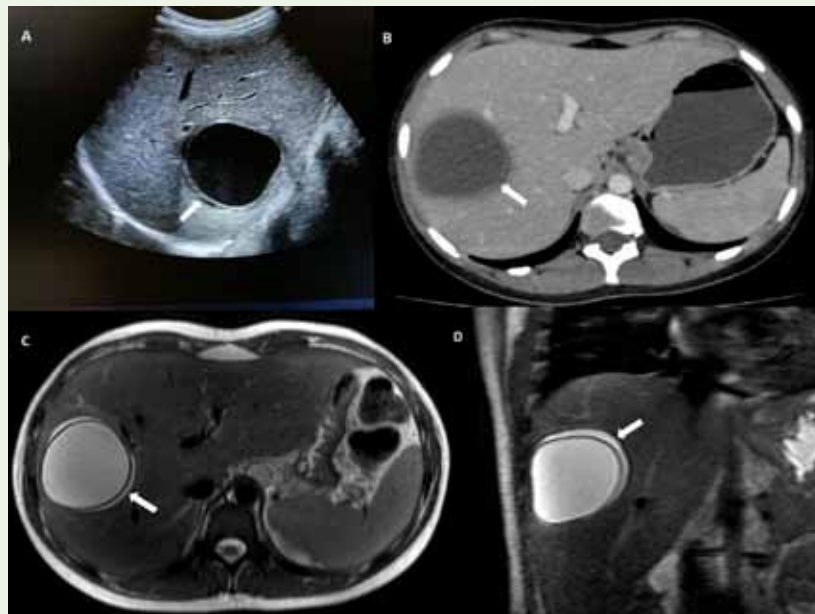


Figure 2: Case of a 19-year-old female with right hypochondriac pain: Ultrasound image of the liver (Image A) shows an anechoic double-walled cystic lesion – ‘Double line sign’ (marked by white block arrow). Image B is the axial section of the contrast-enhanced CT abdomen of the same patient showing a rounded well-defined non-enhancing hypodense double-walled cystic lesion (marked by a white arrow). Axial (Image C) and coronal sections (Image D) of the T2-weighted MR sequence reveal a similar double-walled (marked by a white arrow) hyperintense cystic lesion in the right lobe of liver.

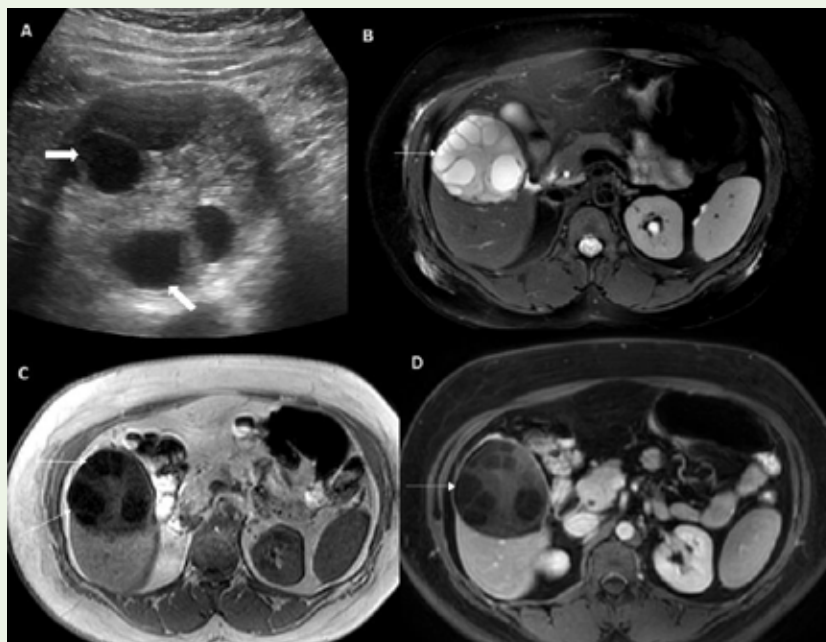


Figure 3: Case of a 37-year-old female with fever: Image A is an ultrasound image of the liver showing a well-defined hyperechoic lesion with few anechoic cystic lesions (marked by white block arrow), suggestive of daughter cysts (WHO stage CE-3B or Gharbi type II). Axial sections of T2-weighted (Image B), T1-weighted (Image C), and T1-weighted post-contrast (Image D) sequences of the same patient reveal a multivesicular, well-defined peripherally enhancing partially exophytic lesion with daughter cysts (marked by white line arrow).

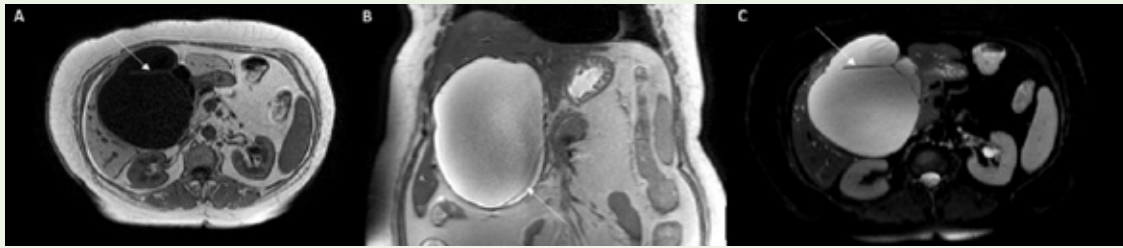


Figure 4: Case of a 56-year-old female with abdominal pain: T1-weighted axial section (Image A) and T2-weighted coronal (Image B) and axial (Image C) section respectively of MRI abdomen reveals a well-defined partially exophytic well-defined T1-hypointense and T2-hyperintense lesion showing few T2 hypointense septae (marked by white line arrow) within (WHO stage CE-2 or Gharbi type III).



Figure 5: Case of a 15-year-old male with right hypochondriac pain: Image A is an ultrasound image of the liver showing a heterogenous lesion with few hypoechoic detached irregular laminated membranes (marked by white block arrow) with hyperechoic matrix- ‘Ball of Wool sign’ suggestive of WHO stage CE-4 or Gharbi type IV. The axial non-contrast section (Image B) of the CT abdomen in the same patient reveals a well-defined hypodense lesion with internal linear calcification within (marked by white line arrow). Image C is a T2-weighted axial section of an MRI abdomen showing a well-defined T2 hyperintense cystic lesion in the liver with a T2 hypointense area (marked by a white line arrow) and few T2 hypointense thin septations (marked by white block arrow) suggestive of detached membranes.

gastrohepatic ligament. Trans-diaphragmatic migration manifests variedly ranging from simple adherence of the cyst to the diaphragm to more severe complications like rupture into the pleural cavity, seeding in the pulmonary parenchyma, and chronic bronchial fistula [1].

Lung

The second most commonly involved organ is the lung which shows spread by hematogenous mode in adults and is probably the most common organ in children [2]. Most cysts are acquired in childhood, remain asymptomatic for a long period, and are usually diagnosed incidentally on chest radiography [1]. Calcification in pulmonary cysts is very rare (0.7% of cases), although it may be seen in pericardial, pleural, and mediastinal cysts [1].

Giant pulmonary hydatid cysts are common in pediatric patients due to their expeditious growth in childhood attributed to the lung tissue and immune system of the host [2]. A unique feature associated with pulmonary hydatid cysts is their change in shape with respiration. The imaging findings vary with the stage of parasitic growth and its relationship with the lung tissue.

Chest radiography is the initial imaging modality to examine patients with pleuropulmonary hydatid disease [7] (Figure 10). The uncomplicated cysts appear as well-defined homogenous radiopacity on chest X-ray (Figure 10). The loss of a spherical shape on an X-ray with the appearance of a small depression (resulting in a reniform shape) may imply bronchial rupture and has been referred to as the “slot sign” [12]. CT is quite effective for visualization of collapsed cyst membranes and daughter cysts as well as chest wall invasion or pleural extension by the cysts.

The growth of the cyst produces erosions in the bronchioles that are included in the pericyst causing it to rupture resulting in communication with the tracheobronchial tree, allowing air to enter the potential space between the pericyst and the ectocyst giving rise to the “meniscus sign” [2]. When communication develops between the tracheobronchial tree and the endocyst, air enters between the endocyst and the pericyst which appears as a radiolucent rim around the cyst known as the “air crescent sign” [12] (Figure 10). The “Cumbo sign” and “double arch sign” are noted with the introduction of more air in the endocyst forming an air-fluid level with accompanying surrounding pulmonary consolidation which indicates expelled cyst

fluid. If air continues to enter the cyst cavity, the two layers separate from each other with the collapsed and crumpled endocyst floating freely in the most dependent part of the pericyst cavity known as the “water lily sign” or the “camolette sign” [12] (Figure 10). After the expectoration of cyst fluid, hyperattenuating collapsed membranes can be seen within the dependent part of the cyst, known as the “whirl sign” or “serpent sign”. After the complete expectoration of the cyst fluid and membranes, the cyst appears only air-filled, known as the “Dry cyst sign” [13].

Brain

Hydatid cyst of the brain is an extremely rare entity, more commonly diagnosed in children. Usually solitary, the hydatid cysts can occur anywhere within the brain, with supratentorial predominance, commonly involving the parietal lobe, especially along the territory of the middle meningeal artery [2].

A well-defined spherical or oval homogeneous cystic lesion with a thin wall and smooth margins is noted on both CT and MRI imaging modalities with imaging characteristics of the cystic component similar to that of CSF [1]. T1 and T2-weighted MR imaging shows a well-defined unilocular lesion with a CSF signal intensity that does not show any diffusion restriction or perilesional edema [7]. The typical MR imaging feature for the pericyst is a hypointense rim on T2-weighted images, however, a hyperintense halo may also be encountered [7]. The presence of surrounding edema and peripheral enhancement on MR imaging indicates either impending rupture or infection.

Calcification is better evaluated on CT; however, it is an uncommon finding for cerebral hydatid. Our case documented calcification within the cerebral hydatid cyst (Figure 11). The most important complications of cerebral hydatidosis are infection and rupture of the cysts. Infected hydatid cysts show contrast enhancement making differential diagnosis difficult [2].

MR imaging is a superior imaging modality to CT in the pre-operative evaluation of cerebral hydatid cysts [7]. Differential diagnoses include arachnoid cysts, porencephalic cysts, epidermoid tumors, pyogenic abscesses, and cystic tumors of the brain. Common complication includes intracerebral rupture with a risk of seedling resulting in local and spinal recurrence [14].

Muscle Involvement

Intramuscular hydatid is a rare entity. The thigh and gluteal region are the most common locations for subcutaneous hydatid cysts (Figure 12), followed by the head and neck region.

Ultrasonography is a crucial non-invasive technique for confirming the diagnosis of hydatid disease, which shows distinctive daughter cysts. The CT appearance of hydatid cysts may sometimes resemble tumors when they present as solid masses, however, diagnosis can be confirmed by the presence of daughter cysts or calcifications within the cyst wall [15] (Figure 12).

MRI is an important imaging modality in diagnosing and evaluating the extent of skeletal muscle infestation. In the muscles, the cysts typically show multiple vesicles within the mother cyst,

secondary to the endogenous proliferation of the germinal layer referred to as a “cyst or cysts within a cyst” [15]. These cysts show a hypointense signal as compared to that of the intra-cystic fluid on T1 and low or high signal intensity on T2-weighted images [15] (Figure 13). A low-signal intensity rim is evident on T2 weighted MR images, referred to as the rim sign, which can be a valuable MRI finding in the diagnosis of muscular hydatidosis and helps to differentiate it from other cystic lesions or tumors in the muscles.

Skeletal Involvement

Bone involvement is one of the rare manifestations of hydatid disease, often misdiagnosed on initial radiological evaluation. The absence of pericyst formation is a defining characteristic of bone hydatid cysts, resulting in the lack of peripheral capsular calcifications, causing an aggressive proliferation in an irregular branching pattern, thus eventually the parasite infiltrates the osseous tissue and erodes the cortex [2].

Radiographs usually reveal a well-defined multi-loculated osteolytic lesion, accompanied by bone expansion, thinning of the cortical bone, and extension into the surrounding soft tissues [7] (Figure 14). Computed tomography (CT) imaging provides improved visualization of lytic lesions, allowing for the distinction between unilocular and multilocular lesions and identifying any extensions into soft tissues [16] (Figure 14). In cases where they exist, characteristic mother and daughter cysts may be observed, resulting in a visual appearance resembling a “rosette” or “spoke wheel” [16]. Parasitized bone has varying signal intensity on T1-weighted MR images, ranging from medium to low, and high signal intensity on T2-weighted images.

Extraosseous HCs have the potential to undergo calcification (Figures 12 & 14), while calcification is uncommon in intraosseous HCs.

Spinal HD is the most common site of bony involvement, most commonly involving the thoracic spine [16]. It can be intramedullary, intradural extramedullary, extradural intraspinal, vertebral, or paravertebral in location [16]. The spine is primarily infested through porto-vertebral shunts, with the centre of the vertebral body being the initial site of involvement. Spinal hydatid disease may mimic tuberculous spondylitis or chronic osteomyelitis [2].

Typical imaging characteristics of spinal HD include the absence of osteoporosis or sclerosis in the affected bone, no involvement of the intervertebral disk space, and the presence of a subperiosteal, subligamentous, or paraspinous extension of the disease [17].

Intraperitoneal and Retroperitoneal Involvement

Peritoneal hydatidosis always occurs secondary to hepatic disease, though some unusual cases of primary peritoneal involvement have been described [18]. Most of the cases are related to previous surgery for hepatic disease, although spontaneous, asymptomatic micro-ruptures of hepatic cysts into the peritoneal cavity are not uncommon (12% of cases) [18].

Ultrasound is the first line of investigation for the demonstration of cystic membranes, septa, and hydatid sand; however, CT is



Figure 6: Case of a 45-year-old patient: Coronal MPR reconstruction of non-contrast (Image A) and contrast phase (Image B) of CT abdomen reveals a well-defined mixed density lesion in the liver showing multiple non-enhancing hypodense detached laminated membranes (marked by white block arrow) with calcified matrix (hyperdense areas on non-contrast phase)- WHO stage CE-4 or Gharbi type IV. Image C is the axial contrast phase section of the CT abdomen showing similar findings.



Figure 7: Case of a 66-year-old male patient with pain in the abdomen: Axial (image A) and its coronal MPR reconstructed sections (Image B) reveal a well-defined hypodense lesion in the right lobe of liver with peripheral calcifications, not showing enhancement on contrast phase (Image C) – WHO stage CE-5 or Gharbi type V lesion. Note should be made of a few dots of calcification at the periphery of the lesion corresponding to scolices or daughter cysts (marked by a white line arrow).

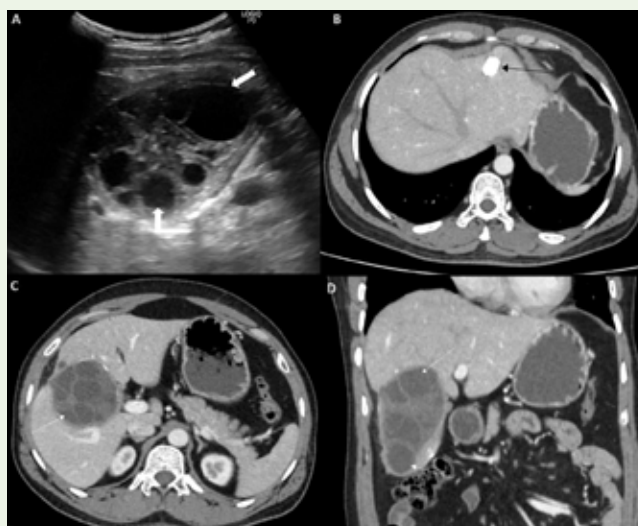


Figure 8: Case of a 38-year-old male patient with right hypochondriacal pain: Image A is an ultrasound image of the liver showing a well-defined hyperechoic lesion with few anechoic cystic lesions (marked by white block arrow), indicative of daughter cysts. This was confirmed on contrast-enhanced CT abdomen axial (Image C) and coronal (Image D) MPR reconstructed sections that revealed a well-defined, lobulated, multiloculated, multi-cystic lesion with septations within and few areas of peripheral calcifications, suggestive of hydatid cyst (WHO stage CE-3B or Gharbi type II). Image B shows a completely calcified lesion (marked by a black line arrow) suggestive of a calcified hydatid cyst (WHO stage CE-5 or Gharbi stage V)

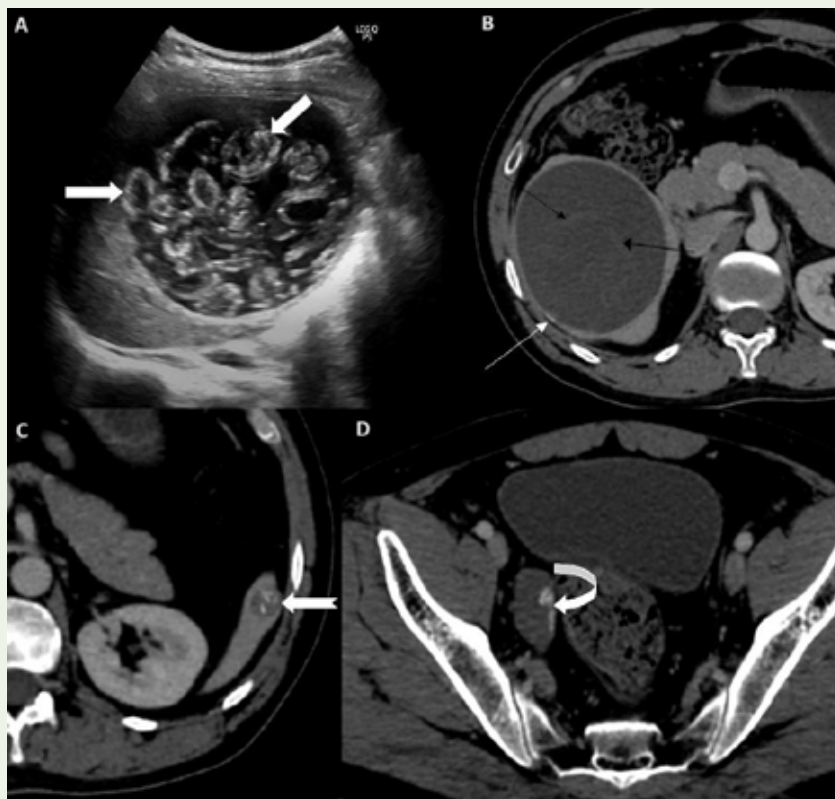


Figure 9: Case of a 40-year-old male patient with pain in the abdomen and fever: Image A is an abdomen ultrasound of the right hypochondriac region showing a cystic lesion with multiple hyperechoic detached laminated membranes within (marked by white block arrow). Image B is an axial section of the contrast-enhanced CT (CECT) abdomen that reveals a well-defined thin-walled hypodense cystic lesion in the liver showing mildly hyperdense floating membranes (marked by black line arrow) within and a foci of wall calcification (marked by white line arrow) suggestive of “Water lily sign” - (WHO stage CE-3A or Gharbi type II). Image C is an axial section of the CECT abdomen showing a well-defined thin-walled cystic lesion with multiple calcific foci within (marked by a white notched arrow), suggestive of splenic hydatid cyst. Image D is an axial section of the CECT abdomen at the bladder that reveals a well-defined thin-walled hypodense cystic lesion with foci of calcification (marked by white curved arrow) in the pelvis on the right side posterior to the bladder, suggestive of pelvic peritoneal hydatid.



Figure 10: Case of a 60-year-old female with cough for 2 months: Contrast-enhanced computed tomography axial section (Image B), and coronal (Image A) and sagittal (Image C) MPR reconstruction reveals a well-defined peripherally enhancing thick-walled cavity with multiple non-enhancing cystic locules with few hyperdense septae/membranes (marked by white block arrow) within.



Figure 11: Case of a 20-year-old female with cough and hemoptysis: Image A is a frontal chest radiography showing a well-defined rounded radio-opacity in the right lower lung zone making an acute angle with the lung. Note should be made of air crescent sign (marked by white block arrow with black margin). Image B is a chest ultrasound showing a hypoechoic cystic lesion in the right lower lung lobe with an undulating membrane (marked by a white line arrow). Axial computed tomography section (Image C) reveals a well-defined peripherally enhancing hypodense cavitory lesion showing fluid and few air pockets within with hyperdense undulating floating membrane (marked by white block arrow) – ‘Water lily sign’. Image D is a coronal MPR reconstruction of the CT chest showing a basal segment bronchus communicating with the cavitory lesion (marked by a white notched arrow) giving rise to a Broncho-cavitory fistula.

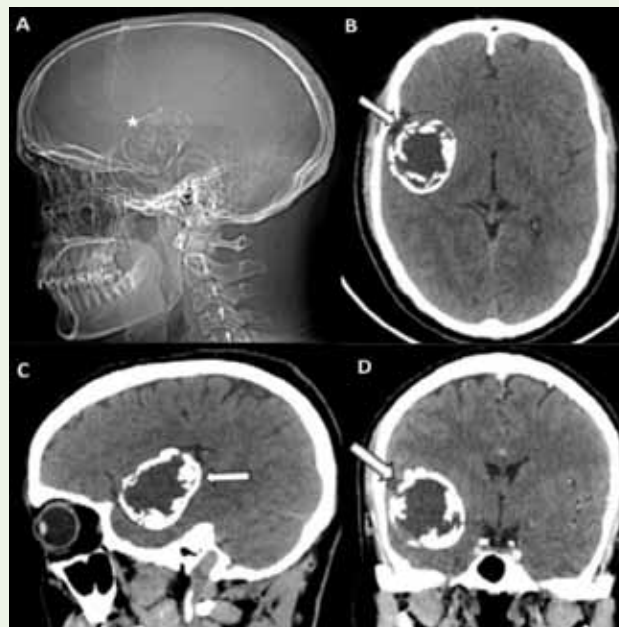


Figure 12: Case of a 36-year-old male with weakness on the left side of the body. Image A is a lateral skull radiograph showing a well-defined radio-opaque (calcified) intracranial lesion (marked by a white star). Computed tomography axial section (Image B) with sagittal (Image C) and coronal (Image D) MPR reconstruction of the brain in soft tissue window reveals a well-circumscribed calcified mass in the anterior temporal region with peripheral arch-like calcification (marked by white arrow).

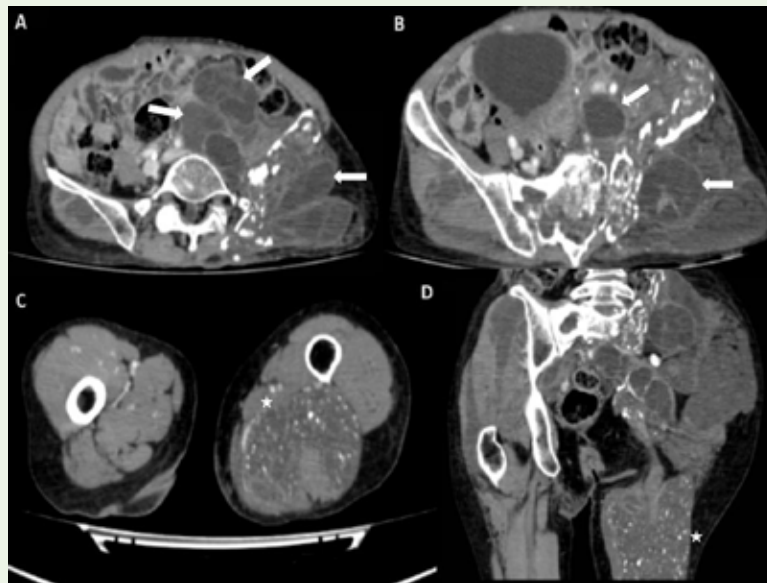


Figure 13: Case of a 60-year-old female with pain in the left lumbar and iliac region: Contrast-enhanced computed tomography axial sections (Image A and B) of the abdomen reveal multiple multi-loculated peripherally enhancing lesions at various stages (marked by white block arrows) noted in bilateral gluteus maximus, left gluteus medius and minimus, left piriformis and iliacus muscle and left obturator externus. Image C is an axial section of contrast-enhanced CT at the level of the proximal femur and Image D is a coronal MPR reconstruction of contrast-enhanced CT at the level of the pelvis and upper thigh of the same patient showing multiloculated cystic lesions with few septations and multiple tiny punctate foci of calcification (marked by white stars) in the left adductor and hamstring muscles.

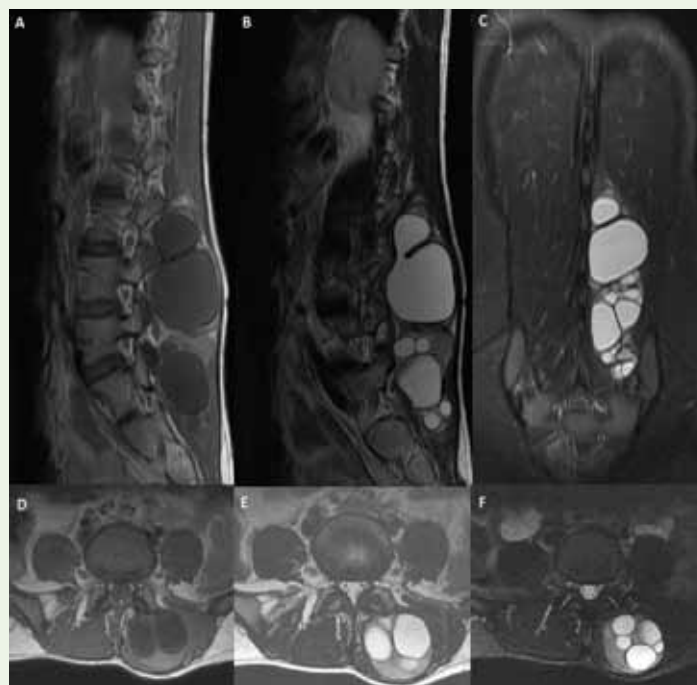


Figure 14: Case of a 21-year-old female with swelling in her lower back and history of dog feces exposure: T1-weighted (Image A) and T2-weighted (Image B) sagittal sections with STIR coronal (Image C) image of MRI lumbar spine reveal multilocular, encapsulated T1 hypointense and T2/STIR hyperintense cystic lesions with regular borders in left paraspinal muscles. Axial sections of T1-weighted and T2-weighted sections (Image D and E respectively) and T2-weighted FATSAT image (Image F) show similar findings.

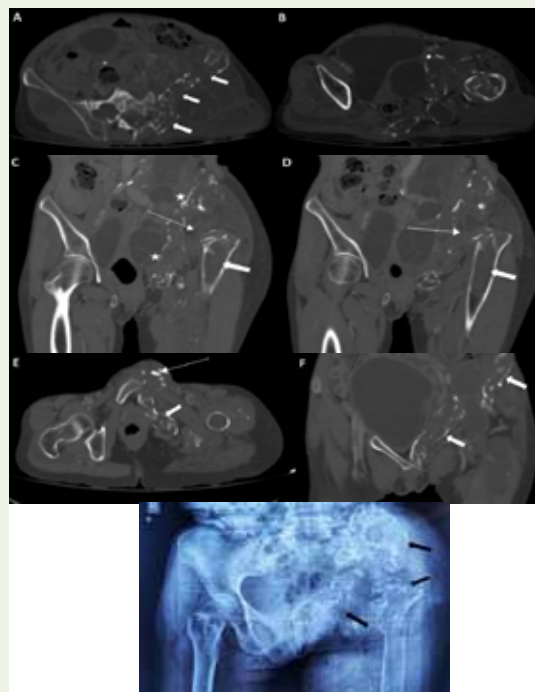


Figure 15: Case of a 52-year-old female presented with left hip pain and limping gait: Images A and B are axial sections of CT abdomen in the bone window showing extensive osteolytic expansile destruction with multiple cortical breaks (marked by white block arrow) and multiple calcific foci in left iliac bone with bony resorption of acetabulum. Coronal MPR reconstruction (Images C and D) of CT pelvis in the bone window of the same patient shows resorption of the left femoral head and superior dislocation of the left proximal femoral (marked by white line arrows) and osteolytic destruction of left iliac bone (marked by white stars). Images C and D also reveal a marrow-replacing lesion in the proximal femoral epiphysis and diaphysis (marked by a white block arrow). Image E is an axial image and Image F is a coronal MPR reconstructed image of the CT pelvis in the bone window that reveals extra-osseous extension of the lesion beyond the pubic rami into the left labia majora where it shows calcification within (marked by white line arrow) and osteolytic destruction (marked by white block arrow). Image G is an Xray pelvis AP view of the patient showing osteolytic destruction of the left half of the pubic bone and left head, neck, and proximal shaft of the humerus (marked by black block arrow) with multiple tiny foci of calcification within the left thigh muscles (marked by black line arrow) indicating muscle involvement.

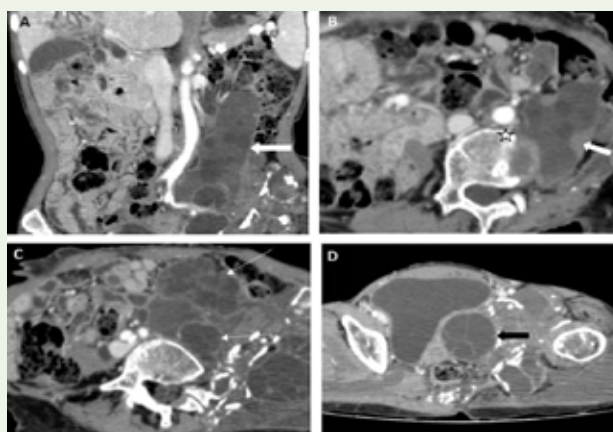


Figure 16: Case of a 52-year-old female diagnosed with disseminated hydatid disease: Axial (Image A) and coronal (Image B) MPR reconstructed images of the venous phase of contrast-enhanced CT abdomen reveal multiple multiloculated varying stages lesions in the retroperitoneum and peritoneal cavity in the left paravertebral region involving left iliopsoas and left quadratus lumborum (marked by white block arrows). Images C and D are axial contrast phase sections of CT abdomen showing multiple multi-loculated varying stage lesions in the left presacral (marked by white line arrow), left peri-vesical (marked by black arrow), and left lumbar region. In Image B, the multiloculated lesion in the left paravertebral region shows osteolytic destruction of the corresponding vertebra (marked by a white star), but no spinal canal involvement.

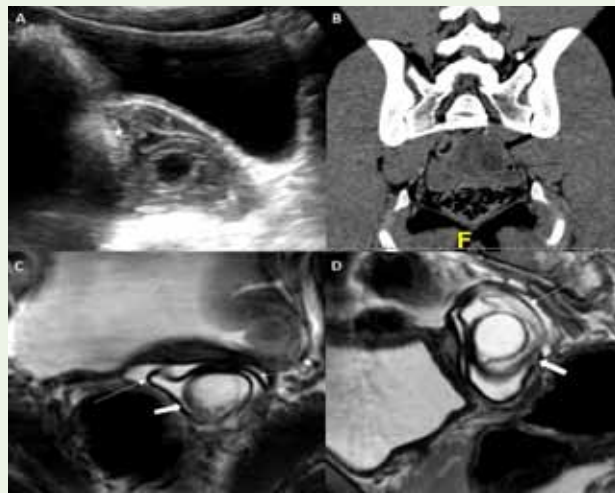


Figure 17: Case of a 24-year-old patient with diagnosed hepatic hydatid disease with incidentally detected pelvic hydatid: Image A is an ultrasound of the pelvis showing a heterogeneously hyperechoic lesion (marked by a white star) with few hypoechogenic laminated membranes within it in the post-vesical region. Coronal MPR reconstructed image (Image B) of non-contrast CT pelvis reveals a well-defined hypodense lesion (marked by black block arrow) with multiple thin internal septations/membranes (marked by black line arrow). Images C and D are T2-weighted axial and sagittal sections of MRI abdomen respectively showing a T2 hyperintense lesion (marked by white block arrow) in the post-vesical region with multiple T2 hypointense septations (marked by white line arrow) within representing crumpled membranes.

the modality of choice in peritoneal seedlings because of better delineation of the extent of disease, cyst wall calcifications, and rupture [18] (Figures 15 & 16). Peritoneal hydatidosis shows imaging features similar to those seen in hydatid disease of other abdominal viscera [7]. Peritoneal hydatid disease may grow and occupy the entire peritoneal cavity, mimicking a multiloculated mass, referred to as an “Encysted Peritoneal Hydatidosis” [1].

The differential diagnosis of peritoneal hydatid disease includes duplication cysts, mesenteric cysts, intraperitoneal abscesses, pancreatic pseudocysts, cystic or myxoid sarcomas, large cystic ovarian tumors, and gossypiboma [7].

Peritoneal dissemination may lead to the implantation of hydatid scolices in several abdominal organs, referred to as “Metastatic hydatidosis” [19]. It may manifest dramatically as a life-threatening condition with anaphylactic shock or acute abdomen due to chemically induced peritonitis [19]. Cysts in this region can grow to enormous sizes spanning craniocaudally along the iliopsoas muscle extending to the extraperitoneal pelvic compartment and may reach up to the inguinal canal and proximal thigh [20].

Conclusion

Hydatid disease is endemic in many parts of the world. Though commonly involves the liver, this parasitic disease can involve almost any organ in our body. Familiarity with both, typical and atypical features of hepatic and extra-hepatic hydatid disease on USG, CT, and MRI can prove advantageous in making prompt diagnosis.

References

- Pedrosa I, Saiz A, Arrazola J, Ferreirós J, Pedrosa CS (2000) Hydatid disease: Radiologic and pathologic features and complications. *Radiographics* 20: 795-817.
- Polat P, Kantarci M, Alper F, Suma S, Koruyucu MB, et al. (2003) Hydatid Disease from Head to Toe 23: 475-494.
- Gharbi HA, Hassine W, Brauner MW, Dupuch K (1981) Ultrasound examination of the hydatid liver. *Radiology* 139: 459-463.
- Inan N, Arslan A, Akansel G, Anik Y, Sarisooy HT, Ciftci E, Demirci A (2007) Diffusion-weighted imaging in the differential diagnosis of simple and hydatid cysts of the liver. *American Journal of Roentgenology* 189: 1031-1036.
- Marti-Bonmati L, Serrano FM (1990) Complications of Hepatic Hydatid Cysts: Ultrasound, Computed Tomography, and Magnetic Resonance Diagnosis. *Gastrointest Radiol* 15: 119-125.
- Greco S, Cannella R, Giambelluca D, Pecoraro G, Battaglia E, et al. (2019) Complications of hepatic echinococcosis: multimodality imaging approach. *Insights Imaging* 10: 113.
- Zalaquett E, Menias C, Garrido F, Vargas M, Olivares JF, Campos D, Pinochet N, Luna A, Dahiya N, Huete A (2017) Imaging of hydatid disease with a focus on extrahepatic involvement. *Radiographics* 37: 901-923.
- Mendez J V, Arrazola J, Lopez GJ, Antela Lopez LJ, Mendez Fernandez A, Ayala AS (1996) Fat-Fluid Level in Hepatic Hydatid Cyst: A New Sign of Rupture into the Biliary Tree? *American Journal of Roentgenology* 167: 91-94.
- Castellanos AA, Granados JFM, Fernandez JE, Muñoz IG, De Asis Triviño Tarradas F (2012) Early phase detection of bile leak after hepatobiliary surgery: Value of Gd-EOB-DTPAenhanced MR cholangiography. *Abdom Imaging* 37: 795-802.
- Kulali F, Acar A, Semiz-Oysu A, Canbak T, Tolan K, Bekte Y (2019) Misleading findings of liver-specific MR contrast agent for radiological diagnosis of cysto-biliary communication in hydatid cysts. *Radiologia Medica* 124: 460-466.
- De J, Choliz1 D, Lecumberri FJ, Franquet OT, Ostiz Zubieta CS (1982) Computed Tomography in Hepatic Echinococcosis. *American Journal of Roentgenology* 139: 699-702.
- Garg MK, Sharma M, Gulati A, Gorski U, Aggarwal AN, Agarwal R, Khandelwal N (2016) Imaging in pulmonary hydatid cysts. *World J Radiol* 8: 581-587.
- Balikian JP, Mudarris FF, D4 M (1974) Hydatid Disease of the Lungs - A

- Roentgenologic study of 50 cases. American Journal of Roentgenology 122: 692-707.
14. Izci Y, Tüzün Y, Seçer HI, Gönül E (2008) Cerebral hydatid cysts: Technique and pitfalls of surgical management. Neurosurg Focus 24: E15.
 15. A. I. García-Díez LHRM, V.M. Villacampa, M. Cózar, M. I. Fuertes (2000) MRI evaluation of soft tissue hydatid disease. Eur Radiol 10: 462-466.
 16. Paruchuri RK, Kapoor A (2020) Osseous Hydatid Disease – A Series of Cases. Indian Journal of Musculoskeletal Radiology 2: 120-124.
 17. Braithwaite PA, Lees RF (1981) Vertebral Hydatid Disease: Radiological Assessment. Radiology 140: 763-766.
 18. Chawla A, Maheshwari M, Parmar H, Hira P, Hanchate V (2003) Imaging features of disseminated peritoneal hydatidosis before and after medical treatment. Clin Radiol 58: 818-820.
 19. Alghofaily KA, Saeedan MB, Aljohani IM, Alrasheed M, McWilliams S, et al. (2017) Hepatic hydatid disease complications: review of imaging findings and clinical implications. Abdominal Radiology 42: 199-210.
 20. Subercaseaux VS, Besa CC, Burdiles OA, Huete GA, Contreras OO (2010) Retroperitoneal hydatid cyst: a common disease in a rare location. Rev Chilena Infectol 27: 556-560.